Foundation University Journal of Engineering and Applied Sciences

FUJEAS
Vol. 6, Issue 1, 2025
DOI:10.33897/fujeas.v6i1.901

Research Article

A Multistage CNN with Branch Concatenation for Classification of Dementia Using MRI Data

Muhammad Shoaib Aslam [a, *], **Memoona Ameer** [b], **Erum Munir** [c]

[a] Department of Information and Communication Engineering, Faculty of Engineering and Technology, The Islamia University of Bahawalpur, Bahawalpur, Pakistan.
[b] Biomedical Engineering Centre, University of Engineering and Technology Lahore, Lahore, Pakistan.
[c] Bahauddin Zakariya University, Multan, Pakistan.

* **Corresponding author**: shoaibaslam499@gmail.com

Article Citation:
Aslam et al. (2025). "A Multistage CNN with Branch Concatenation for Classification of Dementia Using MRI Data". *Foundation University Journal of Engineering and Applied Sciences*
DOI:10.33897/fujeas.v6i1.901

Abstract:

Alzheimer's Disease (AD) is the most common type of dementia and is caused by the accumulation of amyloid-beta plaques in the brain. Worldwide cases of dementia are expected to triple by 2050, which underscores the importance of early diagnosis. In our work, we proposed a multibranched CNN with three concatenations among the branches and tested the method on a dataset accessed from Kaggle. We also implement the SMOTE algorithm on the dataset to overcome class imbalance. The proposed CNN achieved 99.64% accuracy and 99.89% F1-Score on test data and outperformed the various existing methods. The proposed architecture is special because of its ability to extract intricate features at finer levels. The research paves the pathway for improved treatment plans and better prognosis of AD.

Keywords: Alzheimer's Disease; Artificial Intelligence; CNN; SMOTE.

Published by
Foundation University
Islamabad.
Web: https://fui.edu.pk/

1. Introduction

Alzheimer's disease is a neurodegenerative disorder [1], caused by the accumulation of amyloid-beta peptide in the brain [2]. Being the most common type of Dementia [3], it is characterized by cognitive impairment and gradual loss of memory, ultimately disturbing the speech, behavior, spatial orientation, and motor control [4]. The risk of occurrence of AD is highly dependent on genetics [5]. In the USA, AD is now the 6th leading cause of mortality [6]. According to [7], the cases of dementia are expected to increase by three times by 2050.

In addition to amyloid-beta, the other major biomarkers of AD include the phosphorylated tau-protein [8], oxidative stress [9], chronic inflammation induced by microglia [10], changes in composition and dysfunction of membrane lipid metabolism [11], and changes in neurotransmitter pathways [12]. A range of diagnostic procedures has been established with an aim to identify AD in its earlier stages [13]. These include metbolic analysis through mass spectrometery [14], neuroimaging techniques such as MRI [15], PET [16], MRS [17], CT [18], EEG [19] and EvestG [20] etc., Cognitive assessment tools such as Mini Mental State Examination (MMSE) [21] and biomarker assays [22] can also be helpful in identifying the subjects with cognitive impairment.

Due to their non-invasive nature and ability to provide comprehensive

structural, functional, and metabolic features, the neuroimaging techniques are preferred over cognitive assessment tools and biomarker assays [23]. Although neuroimaging modalities are useful, but their manual interpretation is a labor-intensive and time-consuming process, and is sensitive to lack of universality, and subjective errors [24]. Deep learning methods such as CNNs possess a great deal of potential in the analysis of high-dimensional neuroimaging data such as MRI and CT scans [25]. The CNNs can extract underlying intricate patterns in high-dimensional data [26], offer robustness to noise and artefacts [27], can handle multimodal data [28], and are able to automate the analysis procedure with greater efficiency [29].

To advance the field of Computer-Aided Diagnosis Systems and to address the multiclass classification problem of Dementia, we introduce a CNN architecture. The main contributions of our work include:

- Overcoming the class imbalance by using the SMOTE Algorithm [30]
- A novel CNN architecture with multiple branches

The rest of the paper is organized as follows: Related Work provides a brief overview of existing studies on the topic, Materials and Methods section entails the proposed methodology in detail, Results section presents the outcomes of our method and provides a brief comparison to existing methods, while the Discussion and Conclusion sections provide a comprehensive analysis of the study.

2. Related Work

In some studies, EEG data were also used to predict AD [31], but we focused only on the studies using imaging data to predict AD. The authors in [32] used VGG16 with the mRMR algorithm to perform 4-way classification of dementia using 6400 MRI images of the Brain and achieved 98.6% accuracy. Similarly, a VGG16-based transfer learning method in [33] achieved 97.44% accuracy using the same dataset as in [32]. A 12-layer CNN was proposed in [34], trained on the OASIS dataset [35] for AD staging achieved 97.8% accuracy. A novel CNN architecture having two branches, which were trained in parallel using the ADNI [36] dataset, and the outputs were concatenated to further process and perform classification of AD in [37], reached the accuracy value of 99.57% in a 4-way classification problem. A combination of XGBoost, Random Forest, and CNN was used in [38], and the model was trained on the ADNI [5] dataset; their proposed approach maintained the final accuracy of 97.52%. The authors in [39] used deer hunting optimization (DHO) with a pretrained CNN for binary and multiclass classification problems of AD. Their approach attained an accuracy of 96% and 93% for binary and multiclass classification problems, respectively. A CNN built on top of pretrained InceptionV3 was proposed in [40]. CNN in combination with LSTM was used for early prediction of cognitive impairment in [41] using MRI, PET, and neurophysiological data. CNN was combined with the particle swarm optimization (PSO) algorithm in [42] and was trained on ADNI, Kaggle, and a private dataset for AD classification. Combining the handcrafted features and those extracted from GoogleNet, the feed-forward neural network (FFNN) [43] maintained an accuracy of 99.5%.

Although there are promising results presented in the existing studies, there are no restrictions to explore different approaches and architectures for CNNs. The current issues related to AD/ Dementia detection and classification include limited datasets, huge imbalances among classes of data, and the need for more efficient and robust models.

3. Materials and Methods

3.1. Dataset

The dataset used to test the performance of the proposed CNN was accessed from Kaggle. It consisted of a total of 6400 MRI images belonging to four classes divided into train and test sets, and details of class-wise distribution are presented in Table 1. A few images from the dataset are shown below in Figure 1.

Table 1: Class wise distribution

	Mild Demented	Moderate Demented	Non Demented	Very Mild Demented
Train	717	52	2560	1792
Test	179	12	640	448
Total	896	64	3200	2240

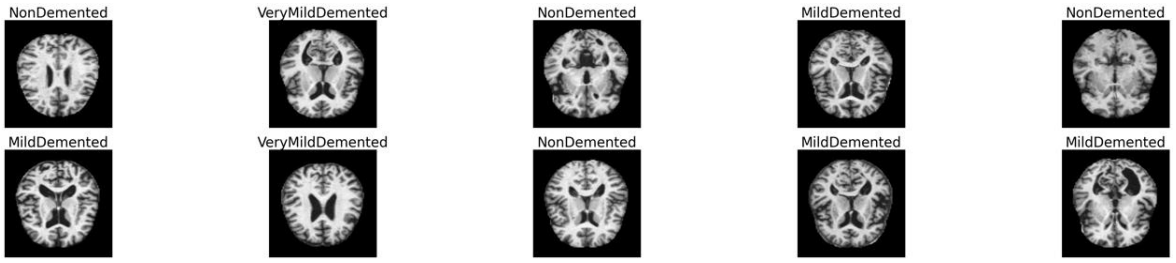

Figure 1: A few sample images from the dataset

3.2. Dataset Preparation Phase

First, the images in the training and testing sets were combined. The sample size of each class and class-wise distribution of data after combining the training and testing folders are demonstrated in Figures 2 and 3.

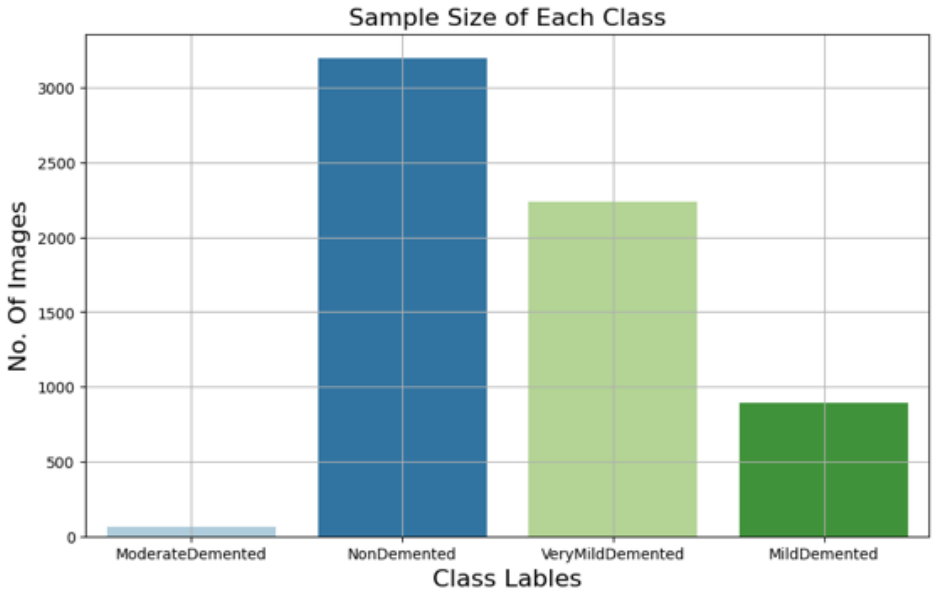

Figure 2: Sample size after combining train and test sets

All the images were rescaled across the color channels, and the color format was converted from BGR to RGB. To keep the uniformity, all images were resized to (176, 176). The main problem with this dataset was the huge imbalances among classes. There are two techniques to overcome this issue. The first one is to downsample the majority classes to match the size of the minority class. In our case, the minority class has only 64 images, so the downsampling would result in a huge loss of data. The second option is to upsample the minority classes to match the size of the majority class or to a set target size [44]. Looking at the challenges of data loss and class imbalances, we adopted the second technique.

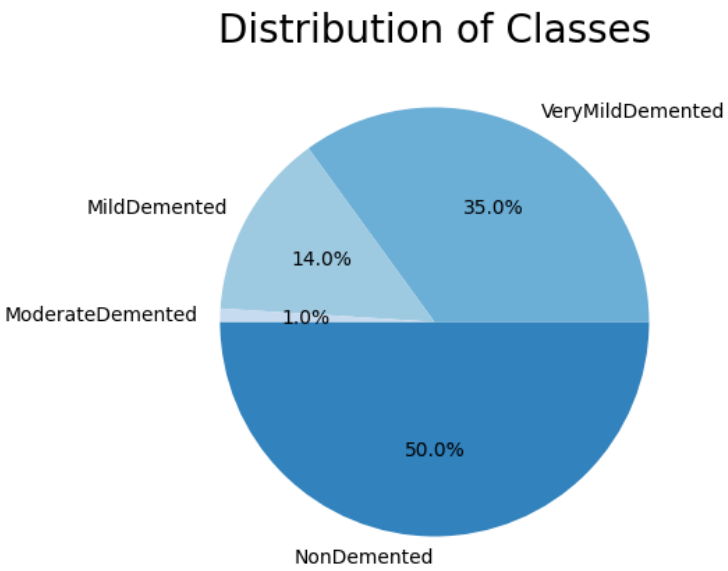

Figure 3: Class-wise distribution of the dataset before upsampling

We used the Synthetic Minority Oversampling Technique (SMOTE) [45] to upsample the minority classes in our data to match the size of the majority class, i.e., 3200 images. The working of the SMOTE algorithm is described here: it first identifies the minority class and selects a random instance for this class. Then, it finds the k-Nearest Neighbors of the selected instance. Then the new instances are synthesized by interpolating between the original instance and its k-Neighbors (k=10, in our case). The synthesized instances are then added to the dataset, thus increasing the volume of data efficiently. SMOTE works on all minority classes until the desired data size is attained.

Figure 4 is the graphical representation of how SMOTE works, and the image was accessed from [46].

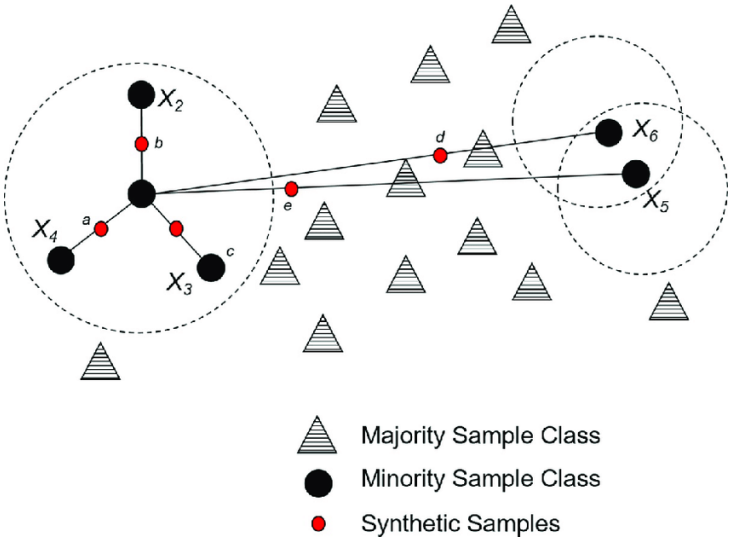

Figure 4: Graphical representation of the SMOTE algorithm

After using the SMOTE method on our chosen dataset, the size of the data increased from 6400 to 12800 images, and each class contained 3200 images, thus resulting in an enhanced and balanced dataset. The same is shown in Figures 5 and 6.

3.3. Data Partitions

After overcoming the issues of a smaller and imbalanced dataset, we split the dataset into train,

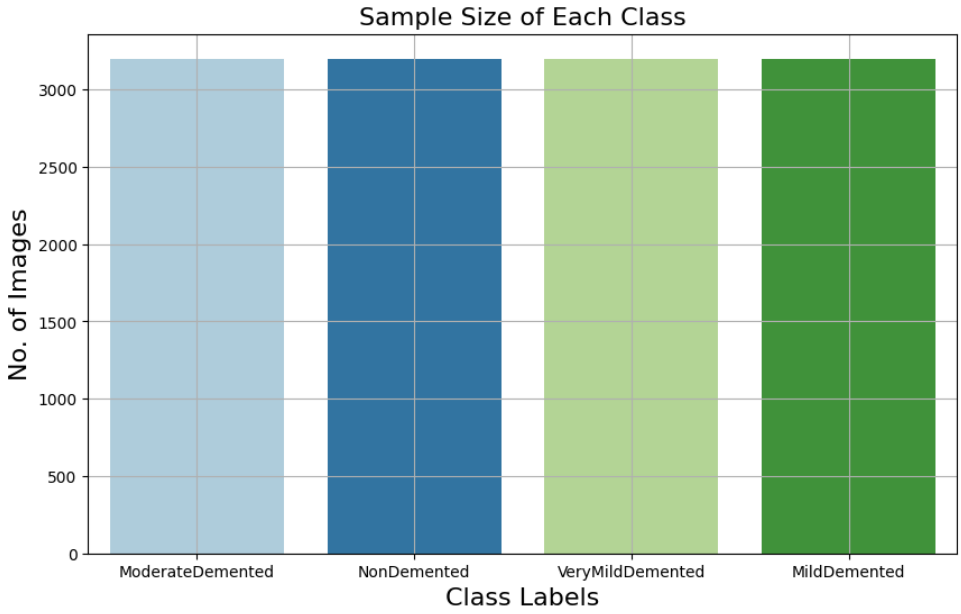

Figure 5: Sample size of each class after upsampling

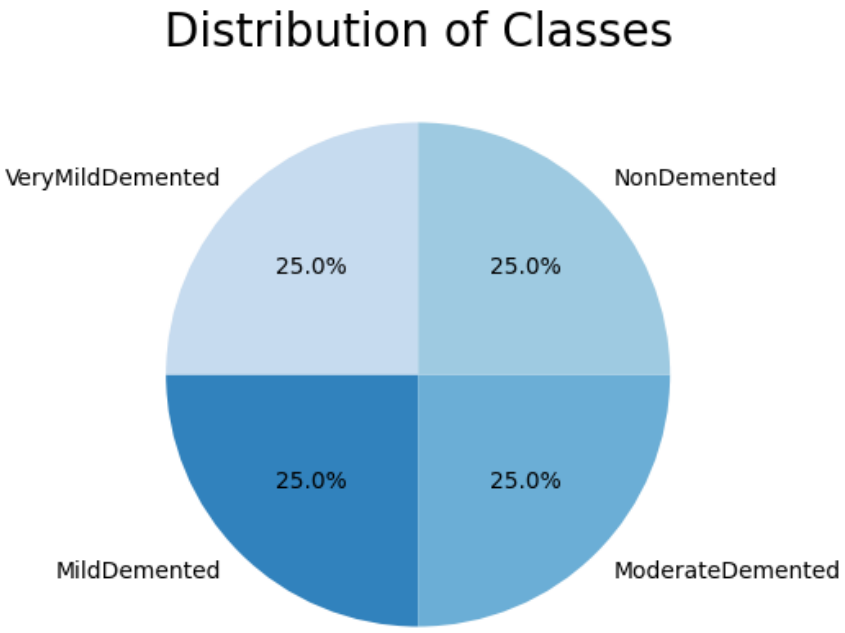

Figure 6: Class-wise distribution of the dataset after upsampling

validation, and test sets. The data partition was carried out in two steps: the first split was used to divide the data in a 70:30 ratio, where 30% data was preserved as a test set. The second split was applied to the 70% data from the first split to equally divide this into two further subsets. One of these subsets was used as a training set, and 2nd subset was used as a validation set. If we look at the data partition method, it is obvious that only 35% of the original data was used for training, and the same percentage was used to validate the training iterations, with the remaining 30% used to test the trained model. The data partition process is represented in Figure 7.

3.4. Architecture of the Proposed CNN

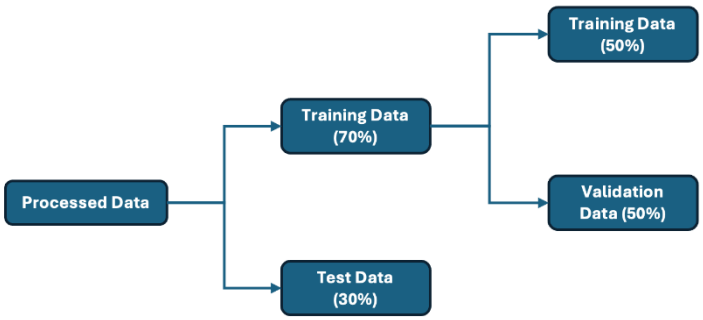

Figure 7: Representation of the data partitions method

The proposed CNN implements multiple steps of feature extraction and concatenation. In the first step,the input training data is fed to two identical branches (branch_1 & branch_2), each having two 2D Convolutional layers and a 2D Maxpooling layer. First convolutional layer uses 32 filters and the second uses 64 filters with the same kernel size of (3,3) in both. Maxpooling layer uses a kernel of size (2,2). The activation used here is ReLU. The outputs from these two self-similar branches are concatenated, and the resulting feature maps are fed to the next phase, where again two branches (branch_3 & branch_4) are trained at the same time on this feature map. The kernel size in Convolutional and Maxpooling layers in these branches is similar to the previous two. Except that branch_3 uses 128 filters and branch_4 uses 256 filters. The outputs from these two are then again concatenated, and the resulting feature map is fed to two further branches (branch_5 and branch_6). The kernel sizes for Convolution and Maxpooling layers in these branches are also similar to the previous ones. Branch_5 uses 128 filters while branch_6 uses 64 filters. The output feature maps from branches 5 and 6 are concatenated, and the final feature vector is passed to a Flatten layer. Following the Flatten layer, there are three Dense layers having 512, 256, and 128 neurons, respectively. Finally, a classification layer with 4 neurons and SoftMax activation is incorporated, which completes the model. The model is compiled using 'adam' optimizer, and 'categorical cross-entropy loss' with Accuracy and F1-Score as performance metrics. Upon compilation, the model gets 34083204 trainable parameters. The model architecture is shown in Figure 8.

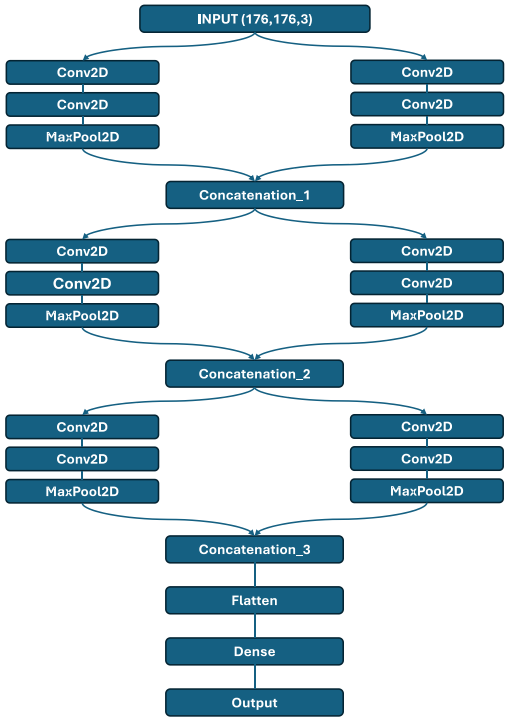

Figure 8: Architecture of the proposed cnn

3.5. Training Setup

The proposed model was trained for 100 iterations/ epochs, where each training iteration was completed in 280 steps, and input data was fed in batches, each consisting of 32 images. Each training iteration was validated by using a sample of data from the validation set. Categorical Cross Entropy Loss, Accuracy Score, and F1-Score were monitored throughout the training period. The hyperparameters of the proposed CNN are given in Table 2.

Table 2: Hyperparameters for the proposed CNN

Hyperparameters	
Activation	ReLU
Optimizer	Adam
No. of Epochs	100
Classification	SoftMax
Loss Function	Categorical Cross Entropy

The methodology implemented in our study is represented in the following diagram, as shown in Figure 9.

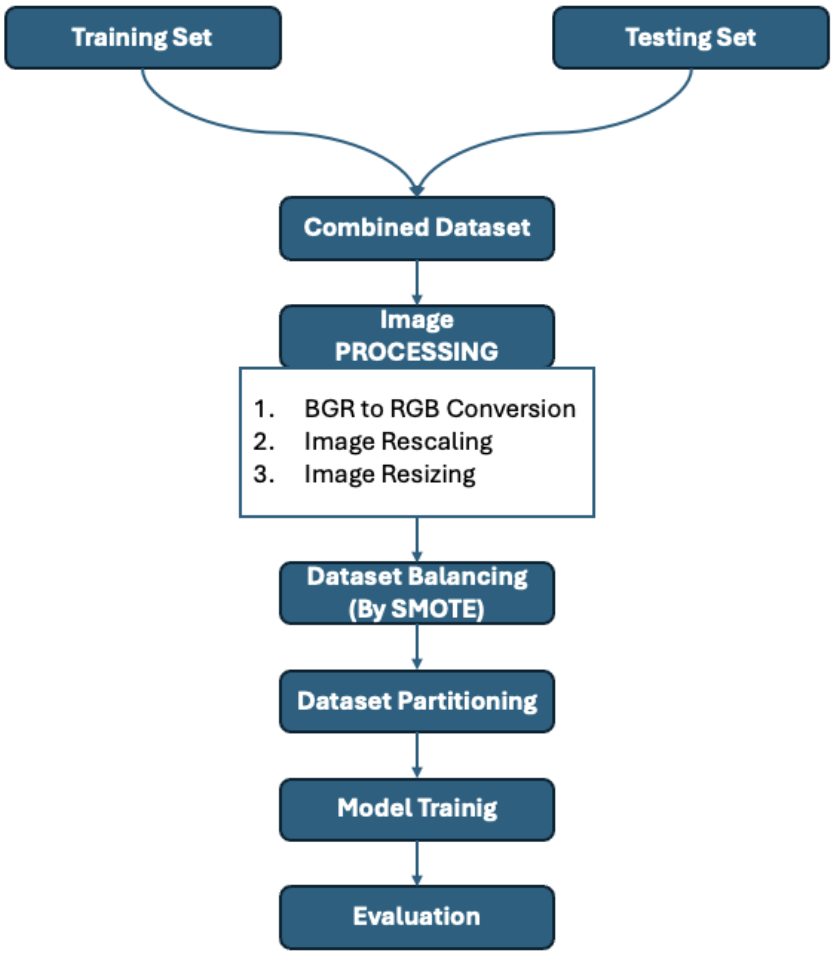

Figure 9: Representation of the proposed methodology

4. Results

4.1. Performance Evaluation

The performance evaluation of the model after 100 iterations of training is summarized in Table 3.

Table 3: Model evaluation metrics after training for 100 epochs

Performance Evaluation of the Proposed CNN			
	Train	**Val.**	**Test**
LOSS	0.055	0.047	0.0319
ACCURACY	1.00	0.9932	0.9964
F1-SCORE	1.00	0.9932	0.9989

During the training phase, the model maintained the perfect Accuracy and F1-score values (1.00), and the loss value was nearing zero. During the validation phase, the model exhibited the fascinating results as it maintained the accuracy and F1-Score of 0.9932, and the loss Value was 0.047 during this phase. When evaluated on test data, the loss value dropped to 0.0319, model accuracy improved to 0.9964, and the average F1-Score jumped up to 0.9989. The near-perfect values of evaluation metrics for the validation and testing phase and the negligible difference between the corresponding values for the training phase demonstrate the efficiency of our proposed CNN architecture.

4.2. Learning Curves

The learning curves for Model Loss and Model Accuracy were generated to interpret how well the model performed during the course of training. Learning curves for model accuracy and model loss during training and validation steps are presented in Figure 10.

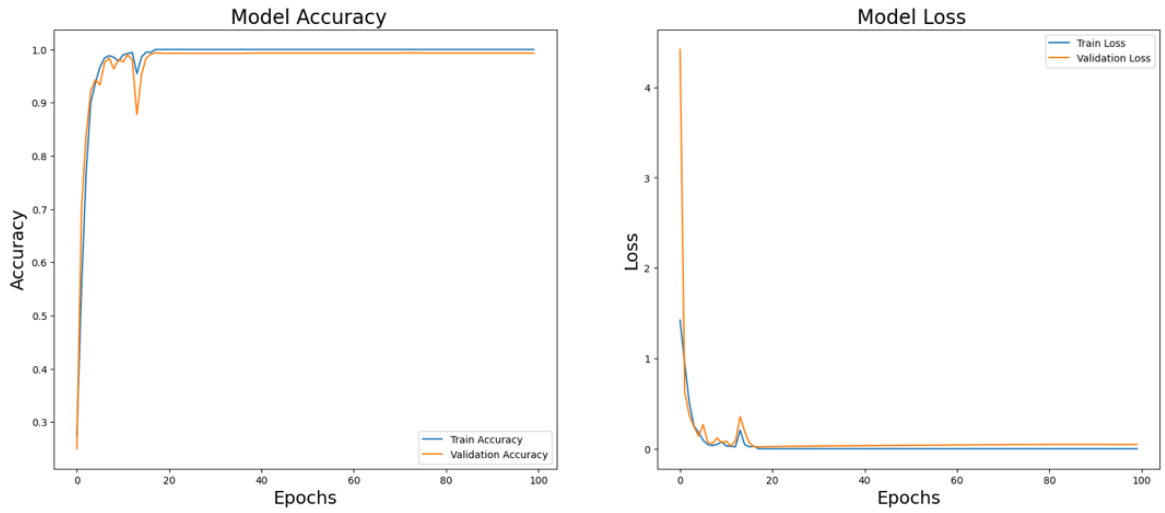

Figure 10: Model accuracy and loss for training and validation

4.3. Confusion Matrix

The confusion matrix was also generated to closely monitor the performance of the CNN for individual classes and monitor the false positives on test data. There were a total of seven false positive

predictions, one for the Mild Demented Class, one for the Non Demented Class, and five for the Very Mild Demented Class. Confusion matrix is shown in Figure 11.

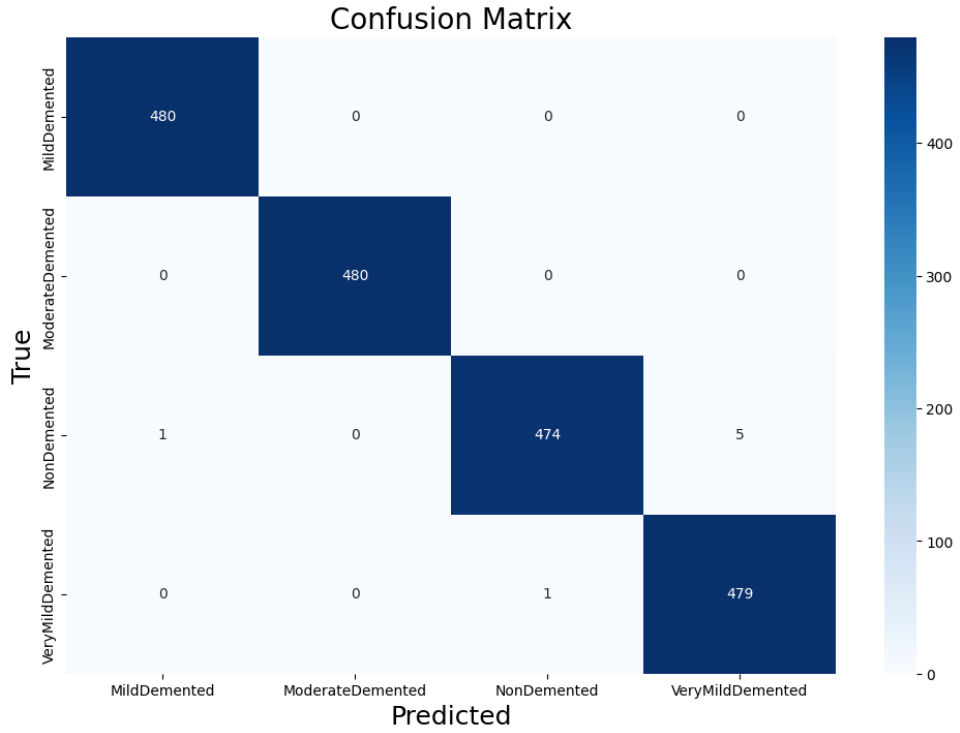

Figure 11: Confusion matrix

4.4. Class-wise Performance Metrics

The confusion matrix was further evaluated to determine the Precision, Recall, and F1-score values for each class. These class-wise performance metrics for the proposed CNN are summarized in Table 4.

Table 4: Class-wise evaluation metrics

Class	Precision	Recall	F1-Score
Mild Demented	0.9979	1.00	0.9990
Moderate Demented	1.00	1.00	1.00
Non-Demented	0.9979	0.9875	0.9927
Very Mild Demented	0.9897	0.9879	0.9938

4.5. Comparison with State-of-the-Art

To evaluate how well our model performed, a comparison against the existing studies was conducted in terms of the performance evaluation metrics and is summarized in Table 5.

5. Discussion

After assessing the model's performance and conducting a comprehensive comparison against the existing methods, it was revealed that the proposed model is capable of precisely differentiating between four stages of dementia. Various studies have introduced different models for staging the problem of dementia and categorizing AD. The exceptional results of our method highlight the

Table 5: Comparison of the proposed approach with existing studies

Year and Ref.	Method	Dataset	Results
2024 [32]	VGG16 + mRMR	Kaggle (6400 MRI Images)	Acc. = 98.59 Sensitivity = 98.78 Precision = 99.01 F1-Score = 98.89
2023 [33]	VGG16	Kaggle (6400 MRI Images)	Acc. = 97.44% Precision = 97.46% Recall = 97.49% F1-Score = 97.48%
2023 [34]	CNN	OASIS	Acc. = 97.8% F1-Score = NOT REPORTED
2024 [37]	Dual-Branch CNN	ADNI	Acc. = 99.57% Precision = 99.57% Recall = 99.57% F1-Score = NOT REPORTED
2023 [38]	XGBoost + RF + CNN	ADNI	Acc. = 97.52% Sensitivity = 97.6%% F1-Score = NOT REPORTED
2023 [39]	CapsNet + DHO	ADNI	Acc. = 96% F1-Score = NOT REPORTED
2023 [40]	InceptionV3	Kaggle (6400 MRI Images)	Acc. = 97.31% F1-Score = 97.05%
2023 [41]	CNN + LSTM	MRI, PET	Acc. = 98.51% Precision = 94.8% Recall= 98% F1-Score = NOT REPORTED
2023 [42]	CNN + PSO	ADNI Kaggle Private	Acc. = 98.50% Acc. = 98.83% Acc. = 97.12% F1-Score = NOT REPORTED
2023 [43]	GoogleNet + CNN	Kaggle (6400 MRI Images)	Acc. = 99.50% Precision = 99.33% Sensitivity = 99.39% F1-Score = NOT REPORTED
Our Study	Multi-Stage CNN with Layer Concatenation	Kaggle (6400 MRI Images)	Acc. =99.64 F1-Score = 99.89%

importance of DL in computer-aided diagnosis systems. The key factor behind the near-perfect results was feature extraction at various levels and the use of different numbers of filters in parallel branches, which makes the model capable of extracting features at both the coarser and the finer levels, thus extracting most of the useful information hidden in the high-dimensional MRI scans.

The proposed architecture presents several advantages over the existing models in published literature. Where most of the studies focus on a binary classification problem, we performed a 4-way classification with an overall accuracy of 0.9964. Our focus was to distinguish between early stages of dementia, which seems difficult, as there are no major visual differences shown on imaging data that can be interpreted by the human eye. While using only 35% volume of the total data for training, the model was able to extract and learn enough information so that it produced satisfying results. The first two self-similar branches allow the collection of a large set of features, which are then processed by the following branches, which compute and extract meaningful information at multiple levels of complexity. Branch_3 used 128 filters, and branch_4 used 256 filters, thus processing information at two different levels. Branch_5 used 128 filters and branch_6 used 64 filters, thus again allowing two levels of information extraction in parallel, resulting in a diversified set of features. Moreover, our proposed architecture is highly modifiable; for example, one can evaluate by using a different number of filters and different kernel sizes staying within the same architecture. Also, the architecture can be extended by increasing the depth of each branch, thus enabling researchers to try different depth levels of feature extraction.

However, the proposed method has some limitations. The dataset used in our study may not capture

the population variety, scanner variation, and acquisition protocols, so the proposed model needs to be tested on other datasets available. Such complex architectures can lead to increased computational costs and require more time to process the data. The processing of the same input at two levels in parallel may lead to overfitting, which can be overcome by using an enhanced volume of validation data and using shuffle to make sure the model doesn't train on the same set of images during various steps of training iteration.

Overall, the proposed architecture advances the field of computer-aided diagnosis systems and is highly capable of assisting in early and precise diagnosis, which leads to better prognosis and enhanced patient outcomes.

6. Conclusion

Our study presents a novel architecture of CNN for 4-way classification of AD/ dementia, by training on brain MRI data. The aim was to extract most of the meaningful features from structural and spatial domains at various levels of complexity, for analyzing the patterns related to AD. Experimental evaluation and comprehensive comparison to the existing studies demonstrated the effectiveness of our method. We achieved an overall accuracy of 0.9964, thus significantly surpassing the existing methods. In conclusion, this research paves the way for further research to find improved treatment plans and enhanced patient outcomes. The future studies should be focused on validating the architecture on other diseases, and also, the modifications should be made to the architecture, keeping in view the nature of the data.

7. References

[1] R. B. Maccioni, J. P. Muñoz, and L. Barbeito, "The molecular bases of Alzheimer's disease and other neurodegenerative disorders," *Arch Med Res*, vol. 32, no. 5, pp. 367–381, 2001.

[2] D. J. Selkoe, "Alzheimer's disease results from the cerebral accumulation and cytotoxicity of amyloid\beta-protein," *Journal of Alzheimer's Disease*, vol. 3, no. 1, pp. 75–82, 2001.

[3] A. L. Fymat, "Dementia: A review," *J. Clin Psychiatr Neurosci*, vol. 1, no. 3, pp. 27–34, 2018.

[4] M. W. Albers et al., "At the interface of sensory and motor dysfunctions and Alzheimer's disease," *Alzheimer's & Dementia*, vol. 11, no. 1, pp. 70–98, 2015.

[5] R. E. Tanzi, "The genetics of Alzheimer disease," *Cold Spring Harb Perspect Med*, vol. 2, no. 10, p. a006296, 2012.

[6] B. D. James, S. E. Leurgans, L. E. Hebert, P. A. Scherr, K. Yaffe, and D. A. Bennett, "Contribution of Alzheimer disease to mortality in the United States," *Neurology*, vol. 82, no. 12, pp. 1045–1050, 2014.

[7] P. Scheltens et al., "Alzheimer's disease," *The Lancet*, vol. 397, no. 10284, pp. 1577–1590, 2021.

[8] P. Rawat, U. Sehar, J. Bisht, A. Selman, J. Culberson, and P. H. Reddy, "Phosphorylated tau in Alzheimer's disease and other tauopathies," *Int J Mol Sci*, vol. 23, no. 21, p. 12841, 2022.

[9] W. Huang, X. I. A. Zhang, and W. Chen, "Role of oxidative stress in Alzheimer's disease," *Biomed Rep*, vol. 4, no. 5, pp. 519–522, 2016.

[10] I. Blasko, M. Stampfer-Kountchev, P. Robatscher, R. Veerhuis, P. Eikelenboom, and B. Grubeck-Loebenstein, "How chronic inflammation can affect the brain and support the development of Alzheimer's disease in old age: the role of microglia and astrocytes," *Aging Cell*, vol. 3, no. 4, pp. 169–176, 2004.

[11] S. M. de la Monte and M. Tong, "Brain metabolic dysfunction at the core of Alzheimer's disease," *Biochem Pharmacol*, vol. 88, no. 4, pp. 548–559, 2014.

[12] S. G. Snowden et al., "Neurotransmitter imbalance in the brain and Alzheimer's disease pathology," *Journal of Alzheimer's Disease*, vol. 72, no. 1, pp. 35–43, 2019.

[13] A. P. Porsteinsson, R. S. Isaacson, S. Knox, M. N. Sabbagh, and I. Rubino, "Diagnosis of early Alzheimer's disease: clinical practice in 2021," *J Prev Alzheimers Dis*, vol. 8, pp. 371–386, 2021.

[14] M. Zhou et al., "Targeted mass spectrometry to quantify brain-derived cerebrospinal fluid biomarkers in Alzheimer's disease," *Clin Proteomics*, vol. 17, pp. 1–14, 2020.

[15] M. E. MacDonald and G. B. Pike, "MRI of healthy brain aging: A review," *NMR Biomed*, vol. 34, no. 9, p. e4564, 2021.

[16] M. S. Allen, M. Scipioni, and C. Catana, "New Horizons in Brain PET Instrumentation," PET Clin, vol. 19, no. 1, pp. 25–36, 2024.

[17] F. Bottino et al., "In vivo brain GSH: MRS methods and clinical applications," *Antioxidants*, vol. 10, no. 9, p. 1407, 2021.

[18] L. C. P. Croton et al., "In situ phase contrast X-ray brain CT," *Sci Rep*, vol. 8, no. 1, p. 11412, 2018.

[19] F. L. Da Silva, "EEG: origin and measurement," in *EEG-fMRI: physiological basis, technique, and applications*, Springer, 2023, pp. 23–48.

[20] Z. Dastghieb, A. Suleiman, Z. Moussavi, and B. Lithgow, "EVESTG Diagnostic Potentials for Neurodegenerative Disorders," *CMBES Proceedings*, vol. 40, 2017.

[21] Y. M. Choe et al., "MMSE subscale scores as useful predictors of AD conversion in mild cognitive impairment," *Neuropsychiatr Dis Treat*, pp. 1767–1775, 2020.

[22] H. Hampel et al., "Blood-based biomarkers for Alzheimer disease: mapping the road to the clinic," *Nat Rev Neurol*, vol. 14, no. 11, pp. 639–652, 2018.

[23] F. Falahati Asrami, "Neuroimaging biomarkers in Alzheimer's disease," 2017.

[24] V. Kumar et al., "Radiomics: the process and the challenges," *Magn Reson Imaging*, vol. 30, no. 9, pp. 1234–1248, 2012.

[25] J. Egger et al., "Medical deep learning—A systematic meta-review," *Comput Methods Programs Biomed*, vol. 221, p. 106874, 2022.

[26] M. Jogin, M. S. Madhulika, G. D. Divya, R. K. Meghana, and S. Apoorva, "Feature extraction using convolution neural networks (CNN) and deep learning," In *2018 3rd IEEE International Conference on Recent Trends in Electronics, Information & Communication Technology (RTEICT)*, IEEE, 2018, pp. 2319–2323.

[27] J. Djolonga et al., "On robustness and transferability of convolutional neural networks," In *Proceedings of the IEEE/CVF Conference on Computer Vision and Pattern Recognition*, 2021, pp. 16458–16468.

[28] S. R. Stahlschmidt, B. Ulfenborg, and J. Synnergren, "Multimodal deep learning for biomedical data fusion: a review," *Brief Bioinform*, vol. 23, no. 2, p. bbab569, 2022.

[29] H. Yu, L. T. Yang, Q. Zhang, D. Armstrong, and M. J. Deen, "Convolutional neural networks for medical image analysis: state-of-the-art, comparisons, improvement and perspectives," *Neurocomputing*, vol. 444, pp. 92–110, 2021.

[30] R. Blagus and L. Lusa, "SMOTE for high-dimensional class-imbalanced data," *BMC Bioinformatics*, vol. 14, pp. 1–16, 2013.

[31] C. Roncero-Parra, A. Parreño-Torres, R. Sánchez-Reolid, J. Mateo-Sotos, and A. L. Borja, "Inter-hospital moderate and advanced Alzheimer's disease detection through convolutional neural networks," *Heliyon*, vol. 10, no. 4, 2024.

[32] M. E. Sertkaya, B. Ergen, M. Türkoğlu, and Ö. Tonkal, "Accurate diagnosis of dementia and Alzheimer's with deep network approach based on multi-channel feature extraction and selection," *Int J Imaging Syst Technol*, vol. 34, no. 3, p. e23079, 2024.

[33] D. A. Arafa, H. E.-D. Moustafa, H. A. Ali, A. M. T. Ali-Eldin, and S. F. Saraya, "A deep learning framework for early diagnosis of Alzheimer's disease on MRI images," *Multimed Tools Appl*, vol. 83, no. 2, pp. 3767–3799, Jan. 2024, doi: 10.1007/s11042-023-15738-7.

[34] Smt. S. Shastri, A. Bhadrashetty, and S. Kulkarni, "Detection and Classification of Alzheimer's Disease by Employing CNN," *International Journal of Intelligent Systems and Applications*, vol. 15, no. 2, pp. 14–22, Apr. 2023, doi: 10.5815/ijisa.2023.02.02.

[35] D. S. Marcus, T. H. Wang, J. Parker, J. G. Csernansky, J. C. Morris, and R. L. Buckner, "Open Access Series of Imaging Studies (OASIS): Cross-sectional MRI Data in Young, Middle Aged, Nondemented, and Demented Older Adults," *J Cogn Neurosci*, vol. 19, no. 9, pp. 1498–1507, Sep. 2007, doi: 10.1162/jocn.2007.19.9.1498.

[36] C. R. Jack et al., "The Alzheimer's disease neuroimaging initiative (ADNI): MRI methods," *Journal of Magnetic Resonance Imaging*, vol. 27, no. 4, pp. 685–691, Apr. 2008, doi: 10.1002/jmri.21049.

[37] A. M. El-Assy, H. M. Amer, H. M. Ibrahim, and M. A. Mohamed, "A novel CNN architecture for accurate early detection and classification of Alzheimer's disease using MRI data," *Sci Rep*, vol. 14, no. 1, p. 3463, Feb. 2024, doi: 10.1038/s41598-024-53733-6.

[38] G. P. Shukla, S. Kumar, S. K. Pandey, R. Agarwal, N. Varshney, and A. Kumar, "Diagnosis and Detection of Alzheimer's Disease Using Learning Algorithm," *Big Data Mining and Analytics*, vol. 6, no. 4, pp. 504–512, Dec. 2023, doi: 10.26599/BDMA.2022.9020049.

[39] S. Venkatasubramanian, J. N. Dwivedi, S. Raja, N. Rajeswari, J. Logeshwaran, and A. Praveen Kumar, "Prediction of Alzheimer's Disease Using DHO-Based Pretrained CNN Model," *Math Probl Eng*, vol. 2023, pp. 1–11, Jun. 2023, doi: 10.1155/2023/1110500.

[40] M. M. Rana et al., "A robust and clinically applicable deep learning model for early detection of Alzheimer's," *IET Image Process*, vol. 17, no. 14, pp. 3959–3975, Dec. 2023, doi: 10.1049/ipr2.12910.

[41] P. Balaji, M. A. Chaurasia, S. M. Bilfaqih, A. Muniasamy, and L. E. G. Alsid, "Hybridized Deep Learning Approach for Detecting Alzheimer's Disease," *Biomedicines*, vol. 11, no. 1, p. 149, Jan. 2023, doi: 10.3390/biomedicines11010149.

[42] R. Ibrahim, R. Ghnemat, and Q. Abu Al-Haija, "Improving Alzheimer's Disease and Brain Tumor Detection Using Deep Learning with Particle Swarm Optimization," *AI*, vol. 4, no. 3, pp. 551–573, Jul. 2023, doi: 10.3390/ai4030030.

[43] A. Khalid, E. M. Senan, K. Al-Wagih, M. M. A. Al-Azzam, and Z. M. Alkhraisha, "Automatic Analysis of MRI Images for Early Prediction of Alzheimer's Disease Stages Based on Hybrid Features of CNN and Handcrafted Features," *Diagnostics*, vol. 13, no. 9, p. 1654, May 2023, doi: 10.3390/diagnostics13091654.

[44] S. Sharma, C. Bellinger, B. Krawczyk, O. Zaiane, and N. Japkowicz, "Synthetic Oversampling with the Majority Class: A New Perspective on Handling Extreme Imbalance," In *2018 IEEE International Conference on Data Mining (ICDM)*, IEEE, Nov. 2018, pp. 447–456. doi: 10.1109/ICDM.2018.00060.

[45] N. V. Chawla, K. W. Bowyer, L. O. Hall, and W. P. Kegelmeyer, "SMOTE: Synthetic Minority Over-sampling Technique," *Journal of Artificial Intelligence Research*, vol. 16, pp. 321–357, Jun. 2002, doi: 10.1613/jair.953.

[46] K. Teh, P. Armitage, S. Tesfaye, D. Selvarajah, and I. D. Wilkinson, "Imbalanced learning: Improving classification of diabetic neuropathy from magnetic resonance imaging," *PLoS One*, vol. 15, no. 12, p. e0243907, Dec. 2020, doi: 10.1371/journal.pone.0243907.